that $d^{60} > d^{90}$, so that from Eq. 1 $\gamma_{us}^{90}/\gamma_{us}^{30} <$ 5.3. Recent ab initio calculations of γ_{us}^{30} (19) then imply $\gamma_{us}^{90} < 8.85$ J m^{-2}. In the nonuniform field at the crack-like tip, the perfect edge character of the 90° dislocations would, therefore, appear to dominate the nucleation process, explaining why 90° dislocations are nucleated in preference to 60° dislocations (20).

A most surprising feature of Fig. 1 is the secondary dislocation (D2) that arises from the primary dislocation line (D1). We have observed a large number of isolated dislocation junctions consisting of short but multiply branched segments; this observation has led us to the conclusion that an existing dislocation can act as a multiplication source. This idea can also be understood in terms of our crack blunting nucleation mechanism. The partially relaxed islands decorating D1 provide low-energy binding sites for diffusing adatoms and grow preferentially during the annealing process. However, the 90° edge dislocation cannot relieve the stress along the direction of the dislocation line, and this stress will continue to increase as the islands grow in size. This stress is clearly a maximum at the island intersections orthogonal to the dislocation line, as evidenced by the distribution of stress lines (M) visible by weak beam TEM in Fig. 2B. It is therefore valid to consider multiplication as an efficient exploitation of primary nucleation because an existing dislocation line provides a large density of highly stressed island intersections. In order to relieve the stress concentration, D2 must be orthogonal to D1 as observed in Figs. 1 and 2.

The nucleation of 90° dislocations in high-misfit films has been a subject of some controversy because these dislocations are unable to glide to the interface. Various formation mechanisms have been proposed that involve the reaction of 60° dislocations (21, 22). Although it is conceivable that such mechanisms may occur, our observations have revealed a direct nucleation path for 90° dislocations driven by stress concentrations at crack-like instabilities. Furthermore, this mechanism suggests the possibility of the opposite process in thicker films: A 90° dislocation that nucleates away from the interface in the residual strain field of the tip may subsequently decompose into two 60° dislocations, which glide to the interface on different (111) planes under the action of the misfit stress. This will be an activated process requiring a sufficiently thick wetting layer for the decomposition to occur, which explains the stability of the 90° dislocations in our images. Under these circumstances, the critical thickness for dislocation nucleation will depend on the formation kinetics of the crack-like instability geometry defined by Eq. 1.

Dislocation emission at crack-like surface instabilities that develop naturally during the growth of high misfit films can provide insights into the basic physics of subcritical crack growth and crack blunting in a controlled and clean environment. An accurate characterization of the unstable tip geometry based on surface microscopies and a comparison with thermally activated models of dislocation emission should allow the extraction of core parameters or unstable stacking energies. This may lead to advances in our understanding of the brittle-to-ductile transition and to a determination of the chief causes of the fracture and failure of materials in service.

REFERENCES AND NOTES

1. R. J. Asaro and W. A. Tiller, Metall. Trans. 3, 1789 (1972).
2. M. A. Grinfeld, Sov. Phys. Dokl. 31, 831 (1986).
3. D. J. Srolovitz, Acta Metall. 37, 621 (1989).
4. A. J. Pidduck, D. J. Robbins, A. G. Cullis, W. Y. Leong, A. M. Pitt, Thin Solid Films 222, 78 (1992).
5. D. J. Eaglesham and M. Cerullo, Phys. Rev. Lett. 64, 1943 (1990).
6. B. J. Spencer, P. W. Voorhees, S. H. Davies, J. Appl. Phys. 73, 4955 (1993).
7. C. W. Snyder, B. G. Orr, D. Kessler, L. M. Sander, Phys. Rev. Lett. 66, 3032 (1991).
8. J. H. van der Merwe, J. Appl. Phys. 34, 123 (1963).
9. S. V. Kamat and J. P. Hirth, ibid. 67, 6844 (1990).
10. L. B. Freund, Mater. Res. Soc. Res. Bull. 17, 52 (1992).
11. R. Vincent, Philos. Mag. 19, 1127 (1969).
12. J. W. Matthews, ibid. 23, 1405 (1971).
13. AFM images were acquired in the tapping mode (Digital Instruments, Santa Barbara, CA) in a dry, He-filled glove box.
14. TEM was performed on a Philips EM400 microscope operated at 100 keV.
15. W. H. Yang and D. J. Srolovitz, Phys. Rev. Lett. 71, 1593 (1993).
16. D. E. Jesson, S. J. Pennycook, J.-M. Baribeau, D. C. Houghton, ibid., p. 1744.
17. C-H. Chiu and H. Gao, Int. J. Solids Struct. 30, 2983 (1993).
18. J. R. Rice, J. Mech. Phys. Solids 40, 239 (1992).
19. E. Kaxiras and M. S. Duesbery, Phys. Rev. Lett. 70, 3752 (1993).
20. An alternative nucleation mechanism involving the coalescence of two faces of a cusp to trap a hollow dislocation core has been proposed by J. Grilhé [Europhys. Lett. 23, 141 (1993)]. However, it seems likely that in many systems the criteria for crack blunting will be met first before coalescence can occur.
21. J. S. Ahearn and C. Laird, J. Mater. Sci. 12, 699 (1977).
22. S. A. Dregia and J. P. Hirth, J. Appl. Phys. 69, 2169 (1991).
23. We acknowledge helpful discussions with G. E. Beltz. We thank M. F. Chisholm for comments on the manuscript, and we are grateful to A. J. McGibbon for assistance with the figures. This research was sponsored by the Division of Materials Sciences, U.S. Department of Energy, under contract DE-AC05-84OR21400 with Martin Marietta Energy Systems, Inc.

18 November 1994; accepted 24 February 1995

Efficient Oxidative Dechlorination and Aromatic Ring Cleavage of Chlorinated Phenols Catalyzed by Iron Sulfophthalocyanine

Alexander Sorokin, Jean-Louis Séris, Bernard Meunier*

An efficient method has been developed for the catalytic oxidation of pollutants that are not easily degraded. The products of the hydrogen peroxide (H_2O_2) oxidation of 2,4,6-trichlorophenol (TCP) catalyzed by the iron complex 2,9,16,23-tetrasulfophthalocyanine (FePcS) were observed to be chloromaleic, chlorofumaric, maleic, and fumaric acids from dechlorination and aromatic cycle cleavage, as well as additional products that resulted from oxidative coupling. Quantitative analysis of the TCP oxidation reaction revealed that up to two chloride ions were released per TCP molecule. This chemical system, consisting of an environmentally safe oxidant (H_2O_2) and an easily accessible catalyst (FePcS), can perform several key steps in the oxidative mineralization of TCP, a paradigm of recalcitrant pollutants.

Halogenated aromatic compounds are common environmental pollutants because of their halogen content (1). Many of these pollutants can be converted into less dangerous organic products and can be eventually degraded by different microorganisms (1–3). However, some of these chlorinated compounds are extremely persistent in the environment because of their slow degradation by reductive or oxidative enzymatic pathways (4, 5). Systems that can remove halogen substituents from aromatics may produce compounds that can be more easily biodegraded. Efficient chemical catalysts are needed that can oxidatively degrade halogenated phenols, especially industrial effluents that include large amounts of chemicals that can overload the transformation capacity of microorganisms. In this case, the use of chemical catalysts to convert recalcitrant pollut-

A. Sorokin and B. Meunier, Laboratoire de Chimie de Coordination du CNRS, 205 route de Narbonne, 31077 Toulouse Cedex, France.
J.-L. Séris, Elf-Aquitaine, GRL-Biotechnology, Lacq, 64170 Artix, France.

*To whom correspondence should be addressed.

ants to more degradable molecules by microorganisms could be beneficial.

Labat et al. have described the oxidation of TCP, a major pollutant produced by paper mills (6), to 2,6-dichloro-1,4-benzoquinone catalyzed by water-soluble metalloporphyrins (7). The two main limitations of this catalytic system (the rather low activity when H_2O_2 is used and the absence at present of large-scale manufacturing procedures for these biomimetic catalysts) have been circumvented by the successful use of tetrasulfophthalocyanine metal complexes in the catalytic oxidation of polychlorinated phenols by H_2O_2 (8). These catalysts supported on ion-exchange resins provide better catalytic activity and stability in TCP or pentachlorophenol oxidation than the corresponding soluble phthalocyanine catalysts and may be recycled several times without significant loss of catalytic activity (8).

Here we report the identification and the quantitative analysis of the compounds resulting from the oxidative dechlorination and aromatic ring cleavage of TCP catalyzed by an iron complex of 2,9,16,23-tetrasulfophthalocyanine [FePcS and MnPcS were prepared according to (9); see Fig. 1 for structures]. Catalytic oxidations of chlorinated phenols were performed under the following experimental conditions (final concentrations): A typical reaction mixture contained TCP (10^{-2} M, about 2000 parts per million), the catalyst (10^{-4}, 10^{-5}, or 10^{-6} M; catalyst/substrate ratio = 1, 0.1, or 0.01%, respectively) in a mixture of acetonitrile-water (1:3, v/v), and the oxidant (5×10^{-2} M; 5 equivalents of $KHSO_5$ or H_2O_2 with respect to the substrate; the oxidant was the last reagent added). Substrate conversions were monitored by high-performance liquid chromatography (HPLC) [μ-Bondapak C_{18} column, eluent of methanol-water (1:1, v/v), flow rate of 1 ml/min, and ultraviolet detection at 280 nm]. Data on the catalytic oxidation of TCP are summarized in Table 1.

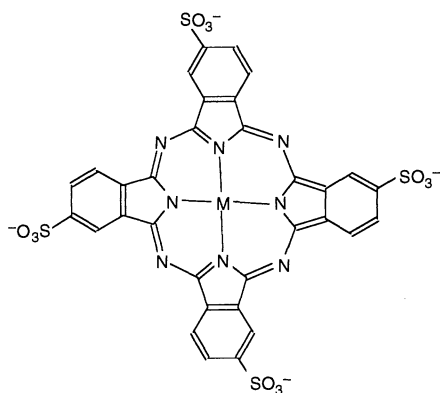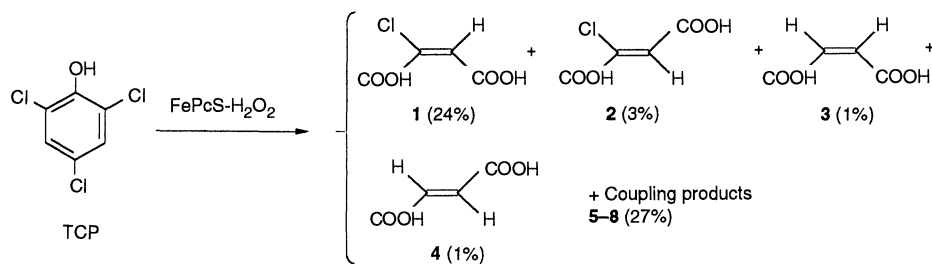In the $KHSO_5$ oxidation of TCP at pH 7,

Fig. 2. Product distribution of the H_2O_2 oxidation of TCP catalyzed by the Fe complex of tetrasulfophthalocyanine (FePcS).

both FePcS and MnPcS catalysts were highly efficient: full substrate conversion was observed within a few minutes even with 0.1% ratios of catalyst to TCP (runs 1 and 6 of Table 1). Our results indicate that (i) high turnover numbers were obtained for the TCP oxidation (for example, with a 0.01% MnPcS/substrate ratio, up to 7000 catalytic cycles were achieved within 5 min), (ii) an environmentally safe oxidant such as H_2O_2 (runs 12 to 14 of Table 1) can be used, and (iii) the initial oxidation product of the TCP oxidation, 2,6-dichloro-1,4-benzoquinone (10), is detected only within the first minutes of the catalytic reaction and then undergoes further oxidative transformations. Labat et al. found that 2,6-dichloro-1,4-ben-

Table 1. Oxidation of TCP by $KHSO_5$ and H_2O_2 mediated by Fe and Mn phthalocyanine complexes FePcS and MnPcS. A typical sample consisted of 20 μmol of TCP (500 μl of a 40 mM stock solution), a catalyst solution [200, 20, or 2 nmol of FePcS or MnPcS for a 1, 0.1, or 0.01% catalyst/substrate (c/s) ratio, that is, 500, 50, or 5 μl of 0.4 mM solution in water, respectively], and a buffered solution of the oxidant (100 μmol of oxidant in 500 μl of buffer, that is, 30.7 mg of $KHSO_5$ or 10 μl of a 35% H_2O_2 solution in water). The reaction medium was adjusted to a final volume of 2 ml with water and stirred at 20°C. Reactions were monitored by HPLC (see text). Phosphate (pH 7), citrate (pH 3), or borate buffers (pH 8.5) were used.

Run	Catalyst	c/s ratio (%)	pH	Conversion (%)	
				1 min	5 min
	KHSO₅ as oxidant				
1	FePcS	0.1	7	97	98
2	FePcS	0.01	7	43	56
3	FePcS	1	2	100	
4	FePcS	0.1	2	96	100
5	FePcS	0.01	2	58	70
6	MnPcS	0.1	7	100	
7	MnPcS	0.01	7	58	73
8	MnPcS	1	2	83	100
9	MnPcS	0.1	2	45	62
10	MnPcS	0.01	2	10	10
11	MnPcS	1	3	100	
	H₂O₂ as oxidant				
12	FePcS	1	7	6	38
13	FePcS	3.7*	7	68	100
14	MnPcS	1	8.5	8	25

*In this case, 740 nmol of FePcS were used (500 μl of a 1.48 M stock solution).

zoquinone was a stable oxidation product in the metalloporphyrin-mediated oxidations of TCP (7). The absence of quinone degradation has been an environmental drawback in the degradation of chlorinated phenols catalyzed by metalloporphyrins.

The product distribution profiles of TCP oxidations depended mainly on the initial concentration of TCP and the substrate/catalyst ratio, as illustrated by the differences in the numbers of Cl^- released during TCP oxidation at different concentrations. These Cl^- concentrations were determined by the mercuric thiocyanate method (11). High dechlorination was observed at low substrate/catalyst ratios, indicating that the degradation of TCP is better suited for dilute solutions than for concentrated solutions (Table 2). The Cl^- release was always greater than one Cl^- per TCP molecule. At a TCP concentration of 2.5 mM, up to 2.1 $\pm$ 0.1 Cl^- per TCP were released. When 2,6-dichloro-1,4-benzoquinone was used as substrate instead of TCP, 100% of substrate conversion was achieved within 3 min with the concomitant release of 0.9 $\pm$ 0.1 Cl^- per quinone molecule.

The Cl^- release data suggested the formation of highly dechlorinated products resulting in possible ring cleavage. To identify these products, we carried out a reaction under experimental conditions correspond-

Table 2. The Cl^- release (molar basis per TCP consumed) associated with the oxidation of TCP by H_2O_2 catalyzed by FePcS. Reaction conditions were identical to those of run 13, Table 1, except for the concentration of substrate. Determinations of Cl^- release were carried out after 1 hour of reaction as on **4** or **5** independent reactions, except as noted.

Run	Substrate (mM)	Number of Cl^- released per TCP
1	2.5	2.12 $\pm$ 0.14
2	5.0	1.96 $\pm$ 0.04
3	5.0*	1.10†
4	7.5	1.73†
5	10	1.74 $\pm$ 0.13

*$KHSO_5$ was the oxidant in this run. †Results of one experiment.

Fig. 1. Structure of sulfonated metallophthalocyanines (MPcS, M = Fe or Mn).

Fig. 3. Analysis of TCP oxidation products in DMSO-d_6 by ^{1}H NMR (250 MHz). Chloroform (CHCl$_3$) was used as the internal standard: **1**, chloromaleic acid; **2**, chlorofumaric acid; **3**, maleic acid; and **4**, fumaric acid. The total yield of coupling products was based on two protons per aromatic ring. Parts per million, ppm.
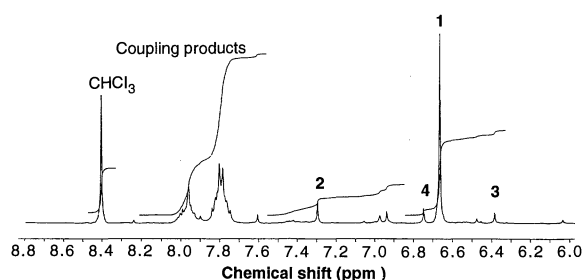
ing to run 13 of Table 1 with H$_2$O$_2$ as the oxidant. After 1 hour of reaction, the reaction mixture was evaporated to dryness and the products of TCP oxidation were extracted with methanol (*12*). This methanolic extract was treated with a trimethylsulfonium hydroxide solution to obtain, in situ during gas chromatography–mass spectrometry (GC-MS) analyses, volatile methyl esters of compounds containing phenolic and carboxylic acid functions (*13*). Four acid derivatives resulting from the oxidative ring cleavage of TCP were identified as methyl esters: chloromaleic acid **1**, chlorofumaric acid **2**, maleic acid **3**, and fumaric acid **4** (Fig. 2). The GC-MS behavior (retention times and mass spectra) of these products were compared with those of authentic samples (*14*). Coupling products **5** and **6** (see below) were also identified by GC-MS as methylated derivatives. The latter compound corresponds to a ring cleavage product of **5**.

To quantify these TCP oxidation products, we analyzed the reaction mixture by proton nuclear magnetic resonance spectroscopy (NMR) (Fig. 3). The ^{1}H NMR spectrum of the extracted reaction mixture [see (*15*) for experimental details] showed the expected signals of **1** ($\delta = 6.66$, 1H), **2** ($\delta = 7.29$, 1H), **3** ($\delta = 6.38$, 2H), and **4** ($\delta = 6.75$, 2H) and two broad signals at $\delta = 7.96$ and $\delta = 7.81$ corresponding to coupling products (see below). We performed the quantitative analysis of TCP oxidation products by using chloroform as the internal standard (product distribution is indicated in Fig. 2). The major product of the oxidative aromatic cycle cleavage of TCP is **1** (yield = 24%), confirming that the catalytic system is able to perform the key steps required for the mineralization of such a chlorinated phenol, that is, dechlorination and cleavage of the aromatic ring. The total yield of identified degradation products was 56%.

We assayed the validity of this extraction method by using a reaction mixture containing 0.125 mmol of each of acids **1** through **4**, but without H$_2$O$_2$. The NMR analysis indicated that 80% of each acid was recovered from the reaction mixture. Taking this into account, we believe that the corrected material balance for the TCP oxidation products was as high as 70%. Furthermore, these identified TCP ring-cleavage products are not the ultimate reaction products. We found that acids **1** through **4** were also oxidized by the catalytic system. When these acids were used as substrates in the reaction mixture instead of TCP (total concentration of equal amounts of the four acids being that of the initial TCP concentration), 40 to 50% of these compounds were converted within 1 hour, under reaction conditions similar to those in which 100% TCP conversion was observed. Consequently, significant amounts of the TCP ring-cleavage products are susceptible to further oxidative degradations.

To fully investigate the oxidation products of TCP (*16*), we isolated the coupling products of TCP oxidation under experimental conditions corresponding to run 13 of Table 1 with a TCP concentration of 10 mM, the reaction volume being 40 ml instead of 2 ml. Any TCP coupling products extractable in organic solvents were isolated and identified by electron ionization–mass spectrometry (EI-MS) (*17*). Three phenolic oligomers resulting from oxidative coupling reactions were identified: phenol dimer **5** and two quinones **7** and **8** (see Fig. 4 for structures). These coupling products were probably formed by reaction of the radical cation derived from TCP after the initial electron abstraction with the excess of unreacted TCP in the reaction mixture. No coupling products were observed in the oxidation of 2,6-dichloro-1,4-benzoquinone. At low TCP concentrations, high dechlorination (Table 2) and low yields of coupling products were observed. These latter phenolic oligomers can be removed from waste water by filtration of water-insoluble precipitates or by the binding of xenobiotics to humus that reduces leaching and transportability of these pollutants, thus limiting their environmental mobility (*18*).

The FePcS-H$_2$O$_2$ system exhibits high catalytic activities, high dechlorination, and the capacity to cleave the ring of chlorinated aromatic derivatives. This catalytic method should be considered as a credible chemical process for the oxidative mineralization of chlorinated phenols and might be useful for the industrial treatment of wastes containing not only polychlorophenols but also other recalcitrant pollutants, such as condensed aromatics.

Fig. 4. Structures of the coupling products identified by mass spectrometry data in the TCP oxidation by FePcS-H$_2$O$_2$.

REFERENCES AND NOTES

1. M. Alexander, *Science* **211**, 132 (1981).
2. M. Häggblom, *J. Basic Microbiol.* **30**, 115 (1990).
3. A. H. Neilson, *J. Appl. Bacteriol.* **69**, 445 (1990).
4. J. A. Bumpus, M. Tien, D. Wright, S. D. Aust, *Science* **228**, 1434 (1985).
5. K. H. G. Verschueren *et al.*, *Nature* **363**, 693 (1993).
6. V. B. Huynh *et al.*, *Tappi* **68**, 98 (1985).
7. G. Labat, J. L. Séris, B. Meunier, *Angew. Chem. Int. Ed. Engl.* **30**, 320 (1991); B. Meunier, *Chem. Rev.* **92**, 1411 (1992).
8. A. Sorokin and B. Meunier, *J. Chem. Soc. Chem. Commun.* 1799 (7 August 1994).
9. J. H. Weber and D. H. Busch, *Inorg. Chem.* **4**, 469 (1965).
10. We monitored and identified 2,6-dichloro-1,4-benzoquinone by HPLC [comparison of its retention time with that of an authentic sample prepared according to the method in (*7*)]. Electron ionization–mass spectrometry data were as follows: 180 [(M+4)$^+$, relative intensity = 45.7, M is the parent peak], 178 [(M+2)$^+$, 100], 176 (M$^+$, 63.2), 150 [(M+2−CO)$^+$, 8.7], 148 [(M−CO)$^+$, 12.6], 143 [(M+2−Cl)$^+$, 5.6], 141 [(M−Cl)$^+$, 12.3], 122 [(M+2−2CO)$^+$, 16.8], 120 [(M−2CO)$^+$, 28.5].
11. K. E. Hammel and P. J. Tardone, *Biochemistry* **27**, 6563 (1988); T. M. Florence and Y. J. Farrar, *Anal. Chim. Acta* **54**, 373 (1971).
12. The reaction mixture (10 ml, experimental conditions corresponding to run 13 of Table 1) was stirred for 1 hour, acidified to pH 2, and dried. The products of TCP oxidation were extracted with methanol (three times with 1 ml). We added 1 ml of 0.1 M Me$_3$S$^+$OH$^−$ in MeOH (Me, methyl) to the methanolic product so-

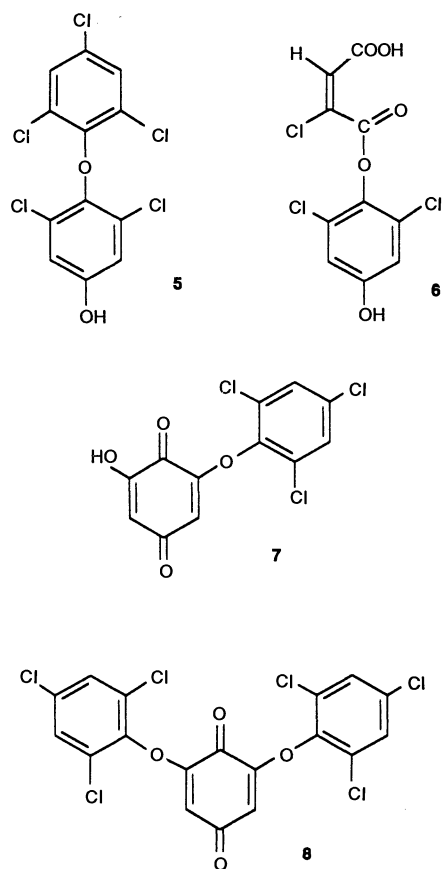lution (13) before GS-MS analysis (Hewlett-Packard 5890, electron-impact ionization at 70 eV). The carrier gas was He, and a 12 m by 0.2 mm HL-1 (crosslinked methylsilicone gum) capillary column was used. The following products were identified as methyl derivatives: chloromaleic acid 1, dimethyl ester, MS data (fragments and relative intensity): 180 [(M+2)$^+$, 2.0], 178 (M$^+$, 5.8), 149 [(M+2−OCH$_3$)$^+$, 33.5], 147 [(M−OCH$_3$)$^+$, 100], 121 [(M+2−COOCH$_3$)$^+$, 1.1], 119 [(M−COOCH$_3$)$^+$, 2.5], 111 [(M−OCH$_3$−HCl)$^+$, 2.1], 59 (COOCH$_3$$^+$, 17.6). Chlorofumaric acid 2, dimethyl ester, MS: 180 [(M+2)$^+$, 3.0], 178 (M$^+$, 10.0), 149 [(M+2−OCH$_3$)$^+$, 33.1], 147 [(M−OCH$_3$)$^+$, 100], 121 [(M+2−COOCH$_3$)$^+$, 3.0], 119 [(M−COOCH$_3$)$^+$, 7.0], 111 [(M−OCH$_3$−HCl)$^+$, 4.0], 59 (COOCH$_3$$^+$, 31.0). Maleic acid 3, dimethyl ester, MS: 144 (M$^+$, 1.1), 113 [(M−OCH$_3$)$^+$, 100], 85 [(M−COOCH$_3$)$^+$, 18.1], 82 [(M−2OCH$_3$)$^+$, 2.8], 59 (COOCH$_3$$^+$, 23.8). Fumaric acid 4, dimethyl ester, MS: 144 (M$^+$, 1.7), 113 [(M−OCH$_3$)$^+$, 100], 85 [(M−COOCH$_3$)$^+$, 71.0], 82 [(M−2OCH$_3$)$^+$, 7.1], 59 (COOCH$_3$$^+$, 41.0). Compound 5, 2,6-dichloro-4-(2,4,6-trichlorophenoxy)phenol, methyl ether, MS: 374 [(M+4)$^+$, 36], 372 [(M+2)$^+$, 58], 370 (M$^+$, 34), 359 [(M+4−CH$_3$)$^+$, 65], 357 [(M+2−CH$_3$)$^+$, 100], 355 [(M−CH$_3$)$^+$, 61]. The distribution pattern of cluster peaks is characteristic of a molecule having five Cl atoms. Compound 6, monoester-dimethyl ether derivative, MS: 342 [(M+4)$^+$, 2.0], 340 [(M+2)$^+$, 5.8], 338 (M$^+$, 5.9), 311 [(M+4−OCH$_3$)$^+$, 5], 309 [(M+2−OCH$_3$)$^+$, 16], 307 [(M−OCH$_3$)$^+$, 18], 283 [(M+4−COOCH$_3$)$^+$, 32.0], 281 [(M+2−COOCH$_3$)$^+$, 93], 279 [(M−COOCH$_3$)$^+$, 100], 175 [C$_6$H$_2$Cl$_2$(OCH$_3$)$^+$, 6.5]. The distribution of peaks in the molecular ion cluster region and in clusters after OCH$_3$ and COOCH$_3$ losses are typical of a molecule with three Cl atoms.

13. W. Butte et al., Anal. Lett. 15, 841 (1982).
14. Maleic and fumaric acids were purchased from Aldrich. Chlorofumaric acid was prepared according to the methods of W. H. Perkin [J. Chem. Soc. 53, 695 (1888)] and M. Akhtar, N. P. Botting, M. A. Cohen, and D. Gani [Tetrahedron 43, 5899 (1987)]. Chloromaleic acid was prepared according to the method of V. G. Gruzdev and G. V. Gruzdev [J. Gen. Chem. USSR 56, 1872 (1986)].
15. The NMR analysis of products of oxidative dechlorination and aromatic cycle cleavage of TCP was performed as for run 2 of Table 2. The reaction mixture (100 ml) was dried in vacuum, and 7 ml of 1 M HCl saturated with NaCl was added to the dry residue. The products were extracted with diethyl ether (three times with 60 ml). After evaporation of the ether extracts, the solid residue was dissolved in deuterated dimethyl sulfoxide (DMSO-d_6) for NMR analysis. We added 6 μl of CHCl$_3$ (0.075 mmol) as an internal standard to quantify the oxidation products. The total yield of coupling products was based on two protons per aromatic ring.
16. Coupling products that have a quinone function cannot be analyzed by GS-MS directly or after treatment with Me$_3$S$^+$OH$^-$.
17. Coupling products of TCP oxidation were also analyzed by EI-MS after separation of organic-soluble material as follows. The reaction conditions were those as for run 13, Table 1. After the reaction mixture had been stirred for 4 min, 40 ml of the violet reaction mixture was treated with CH$_2$Cl$_2$ (four times with 20 ml) and the organic phase was dried. The crude product was extracted with 5 ml of CH$_2$Cl$_2$, and the insoluble material was isolated by filtration. This latter solid residue was soluble in acetonitrile and was identified by EI-MS as 2,6-dichloro-4-(2,4,6-trichlorophenoxy)phenol 5 on the basis of a molecular ion peak cluster typical for a molecule containing five Cl atoms. MS: 360 [(M+4)$^+$, 1.4], 358 [(M+2)$^+$, 3.6], 356 (M)$^+$, 1.3), 290 [(M+4−2Cl)$^+$, 0.7], 288 [(M+2−2Cl)$^+$, 2.8], 286 [(M−2Cl)$^+$, 3.6], 211 (2.1), 209 (6.4), 207 (7.2), 196 (100) (see Fig. 4). After loss of two Cl atoms, the peak distribution indicates a fragment having three Cl atoms. This loss of two Cl atoms suggests that the OH group is in the para position to the diphenyl ether bond. The phenoxyphenol with an OH group ortho to the diphenyl ether bond should show (M−HCl) fragmentation accompanying ring closure (19). We added 12 ml of hexane to the

remaining red-brown CH$_2$Cl$_2$ solution; this produced a red-brown precipitate containing 2-hydroxy-6-(2,4,6-trichlorophenoxy)-1,4-benzoquinone 7, MS: 321 [(M+4−H)$^+$, 2.1], 319 [(M+2−H)$^+$, 8.6], 317 [(M−H)$^+$, 8.8], 301 [(M+2−H$_2$O)$^+$, 4.3], 299 [(M−H$_2$O)$^+$, 3.2], 291 [(M+2−CO)$^+$, 3.2], 289 [(M−CO)$^+$, 4.3], 257 (4.3), 198 (72), 196 (79), 97 (100), a compound containing three Cl atoms. The remaining yellow solution was dried, and succeeding EI-MS analysis showed the presence of 2,6-bis(2,4,6-trichlorophenoxy)-1,4-benzoquinone 8, 500 [(M+4)$^+$, 1.9], 498 [(M+2)$^+$, 3.4], 496 (M$^+$, 1.0), 465 [(M+4−Cl)$^+$, 5.2], 463 [(M+2−Cl)$^+$, 9.0], 461 [(M−Cl)$^+$, 4.8], 319 (53.2), 317 (51.4), 303 (62.8), 301 (60.0), 97 (100), a molecule containing six Cl atoms (Fig. 4).

18. J. M. Bollag, in Degradation of Environmental Pollutants by Microorganisms and Their Enzymes: Metal Ions in Biological Systems, H. Sigel and A. Sigel, Eds. (Dekker, New York, 1992), vol. 28, pp. 205–217.
19. R. E. Clement and H. M. Tosine, Mass. Spectrom. Rev. 7, 593 (1988).
20. This work was supported by Centre National de la Recherche Scientifique, Elf-Aquitaine, and the European Environmental Research Organisation (EERO), Wageningen, Netherlands). A.S. is indebted to EERO (1993) and Elf-Aquitaine (1994) for research fellowships. We thank S. Leppard (on leave from Oxford University) for editing the English of the manuscript.

A Region of Adenylyl Cyclase 2 Critical for Regulation by G Protein βγ Subunits

Jianqiang Chen, Michael DeVivo, Jane Dingus, Anya Harry, Jingrong Li, Jinliang Sui, Donna J. Carty, Jonathan L. Blank, John H. Exton, Robert H. Stoffel, James Inglese, Robert J. Lefkowitz, Diomedes E. Logothetis, John D. Hildebrandt, Ravi Iyengar*

Receptor-mediated activation of heterotrimeric guanine nucleotide–binding proteins (G proteins) results in the dissociation of α from βγ subunits, thereby allowing both to regulate effectors. Little is known about the regions of effectors required for recognition of Gβγ. A peptide encoding residues 956 to 982 of adenylyl cyclase 2 specifically blocked Gβγ stimulation of adenylyl cyclase 2, phospholipase C–β3, potassium channels, and β-adrenergic receptor kinase as well as inhibition of calmodulin-stimulated adenylyl cyclases, but had no effect on interactions between Gβγ and Gα$_o$. Substitutions in this peptide identified a functionally important motif, Gln-X-X-Glu-Arg, that is also conserved in regions of potassium channels and β-adrenergic receptor kinases that participate in Gβγ interactions. Thus, the region defined by residues 956 to 982 of adenylyl cyclase 2 may contain determinants important for receiving signals from Gβγ.

G protein signaling is mediated by both Gα (1) and Gβγ (2) subunits. Effectors regulated by Gβγ include K$^+$ channels, phospholipase C–β, and adenylyl cyclases. Adenylyl cyclases 2 (AC2) and 4 (AC4) are conditionally stimulated by Gβγ (2). Purified AC2 directly interacts with Gβγ (3). Here, we sought to identify regions of AC2 that participate in interactions with Gβγ. Of the eight ACs that have been cloned and expressed (4), two (AC2 and AC4) are stimulated by Gβγ in the presence of activated Gα$_s$, one (AC1) is inhibited by Gβγ, and

J. Chen, M. DeVivo, A. Harry, J. Li, D. J. Carty, R. Iyengar, Department of Pharmacology, Mount Sinai School of Medicine, City University of New York, NY 10029, USA.
J. Dingus and J. D. Hildebrandt, Department of Cell and Molecular Pharmacology, Medical University of South Carolina, Charleston, SC 29425, USA.
J. Sui and D. E. Logothetis, Department of Physiology and Biophysics, Mount Sinai School of Medicine, City University of New York, NY 10029, USA.
J. L. Blank and J. H. Exton, Howard Hughes Medical Institute and Department of Physiology, Vanderbilt University School of Medicine, Nashville, TN 37232, USA.
R. H. Stoffel, J. Inglese, R. J. Lefkowitz, Howard Hughes Medical Institute and Department of Medicine, Duke University Medical Center, Durham, NC 27710, USA.

*To whom correspondence should be addressed.

three (AC3, AC5, and AC6) do not appear to be directly regulated by Gβγ (2, 5). We identified three regions of AC2 that are conserved only between AC2 and AC4 and tested whether peptides corresponding to these regions affected Gβγ regulation of AC2 and other Gβγ-regulated effectors, including K$^+$ channels, phospholipase C–β3 (PLC-β3), β-adrenergic receptor kinase (β-ARK), and AC1.

We synthesized three synthetic peptides corresponding to portions of AC2 (QAID peptide, residues 558 to 569; QEHA peptide, residues 956 to 982; and TEMS peptide, residues 1077 to 1090) and tested their effects on Gβγ stimulation of AC2 (6). AC2 expressed in Sf9 cells was stimulated by Gβγ in the presence of activated Gα$_s$ (2). The QEHA peptide inhibited Gβγ stimulation of AC2 expressed in Sf9 cell membranes; the inhibition of Gβγ stimulation appeared specific because stimulation by mutant (Q227L) activated Gα$_s$ was not affected (Fig. 1A). At all concentrations tested, the QEHA peptide did not affect basal AC2 activity or activity stimulated by Q227L-Gα$_s$ or forskolin (Fig. 1B). Because forskolin still stimulated AC2